

Tentacle probe sandwich assay in porous polymer monolith improves specificity, sensitivity and kinetics

Brent C. Satterfield^{1,2}, Michael R. Caplan^{1,*} and Jay A. A. West³

¹Harrington Department of Bioengineering, Arizona State University Tempe, AZ, ²Cooperative Diagnostics, Greenwood, SC and ³Arcxis Biotechnologies, Pleasanton, CA, USA

Received December 28, 2007; Revised August 18, 2008; Accepted August 19, 2008

ABSTRACT

Nucleic acid sandwich assays improve low-density array analysis through the addition of a capture probe and a specific label, increasing specificity and sensitivity. Here, we employ photo-initiated porous polymer monolith (PPM) as a high-surface area substrate for sandwich assay analysis. PPMs are shown to enhance extraction efficiency by 20-fold from 2 μ l of sample. We further compare the performance of labeled linear probes, quantum dot labeled probes, molecular beacons (MBs) and tentacle probes (TPs). Each probe technology was compared and contrasted with traditional hybridization methods using labeled sample. All probes demonstrated similar sensitivity and greater specificity than traditional hybridization techniques. MBs and TPs were able to bypass a wash step due to their 'on-off' signaling mechanism. TPs demonstrated reaction kinetics 37.6 times faster than MBs, resulting in the fastest assay time of 5 min. Our data further indicate TPs had the most sensitive detection limit (<1 nM) as well as the highest specificity (>1 \times 10⁴ improvement) among all tested probes in these experiments. By matching the enhanced extraction efficiencies of PPM with the selectivity of TPs, we have created a format for improved sandwich assays.

INTRODUCTION

Detection of DNA using conventional probes seems to be inherently limited by a tradeoff between sensitivity and specificity of the assay. For example, sensitivity is typically increased by increasing the affinity of the probe which usually also makes the probe more avid for near neighbors of the targeted sequence (1). Conversely, efforts to increase specificity inevitably include efforts to make the probe less

avid for the near neighbors which typically also make the probe less avid for the targeted sequence thus sacrificing sensitivity. We have previously demonstrated that a cooperative probe can overcome this sensitivity–specificity tradeoff in solution-phase assays, and here we test whether cooperative probes can also break past this tradeoff in a surface-phase hybridization assay. In this work, we utilize a cooperative probe, tentacle probe (TP), in a sandwich assay hybridization at the surface of porous substrate, porous polymer monolith (PPM), to demonstrate proof-of-principle for using cooperative probes in a surface-phase format and to test whether cooperative probes in this surface-phase format can break past the tradeoff between sensitivity and specificity.

For this proof-of-principle, a capillary format is used as it provides relatively rapid kinetics and good fluorescence intensity while requiring relatively small sample volumes. Various efforts to improve extraction efficiency through increasing surface area have been employed including silica beads, microchanneled silica chips, porous metal oxide arrays and agarose films (2–5). Photo-polymerizable monoliths are an alternative method that does not require frits or containment chambers and are cast-to-shape. These structures are formed through a phase separation resulting from a radical-polymerization reaction that is catalyzed by the UV-activated photoinitiator. The resulting polymer material is both monolithic and porous and is easily modifiable with oligonucleotides to enable efficient capture of nucleic acids. They have widely been used in various sample preparation methods, most of these being used in conjunction with capillary electrochromatography or HPLC (6–9). Svec *et al.* (10) have reviewed these materials extensively. In general, PPMs provide high surface area for adsorption of the analyte of interest (11), controllable pore size and porosity based on concentration and type of porogenic solvent (6). In addition, discrete areas of the materials can be spatially located inside the channels through UV-light exposure. They also exhibit good surface adhesion and make even contact with channel walls (12). Although they have been functionalized with

*To whom correspondence should be addressed. Tel: +1 480 965 5144; Fax: +1 480 727 7624; Email: michael.caplan@asu.edu

nucleic acids, they have never been exploited for direct detection of hybridization reactions (13,14).

Nucleic acid sandwich assays deviate from typical array analysis (Figure 1A) through the use of a template-specific labeled probe in a secondary hybridization (Figure 1B), which ideally increases both sensitivity (less background) and specificity (two hybridizations required for detection). One of the first assays of this type was used for the determination of chromosomal location of RNA transcripts (15). Their first application in diagnostics was to detect adenovirus with a limit of detection of 8 attamoles (6×10^5 molecules) (16). Later integration with fluorescence detection removed the necessity of radioactive materials (17).

Recently, Zuo *et al.* (18) used molecular beacons (MBs) to perform direct detection from total RNA. Using their assay, they were able to detect the downregulation of the *c-myc* tumor-associated gene upon cell exposure to anticancer treatments. They were also able to bypass the posthybridization wash step. MBs have a stem-loop structure with a quencher and fluorophore held in close proximity (19). Upon hybridization the stem-loop is opened, extending the fluorophore away from the quencher and causing an increase in fluorescence (20). Although they were originally created for use in real-time PCR, their possession of on-off detection and increased specificity over linear probes makes them attractive as probes in array-based diagnostics as well (21–23).

Ts, similar to MBs with on-off detection, have a stem-loop 'detection' region linked to a linear oligo 'capture' region (1). In general, the target is first bound by the linear capture region, which holds the target in close proximity to the detection region, causing a reaction that is considerably faster than an analogous reaction with a MB (1). The combination of capture and detection regions in a TP additionally provides the cooperative principles from cell targeting (24–28) allowing the construction of highly avid and highly specific probes. We recently reported the

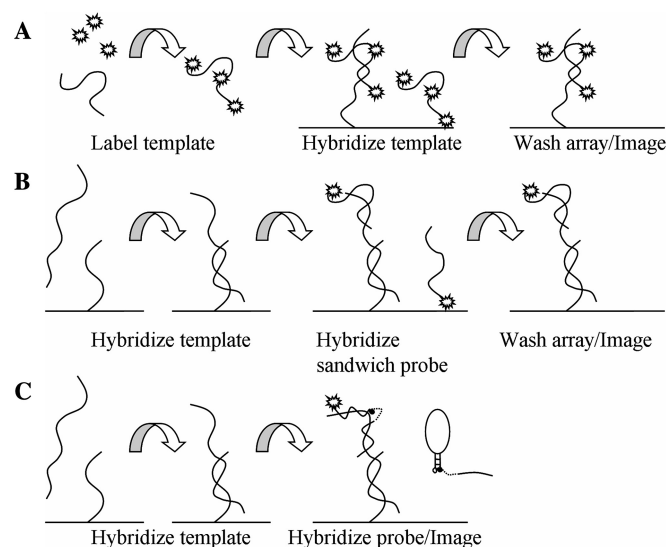


Figure 1. Mechanism of standard hybridization assay (A), standard sandwich assay (B), wash-free sandwich assay with TPs (C). The self-quenching structure of MBs and TPs allows imaging without a wash step.

concentration-independent specificity in a solution-based hybridization reaction (1). In this article, we have applied the TPs hybridization reaction to nucleic acids on a surface to test whether their kinetics and specificity are maintained in a surface-based assay system. We compare the performance of this cooperative probe to several conventional probe technologies (labeled sample, sandwich assay using labeled probe, quantum dot labeled probe and MBs) to provide a broad comparison between conventional probes and this cooperative probe on an identical platform. We assess each probe type's sensitivity (via the wild-type detection limit), specificity (via the ratio of the detection limit for a near neighbor with a single nucleotide polymorphism (SNP) and the wild-type detection), and the time required for the assay to achieve a reasonable result.

MATERIALS AND METHODS

Oligonucleotide synthesis

Probes were designed around the location of a SNP occurring between *Bacillus anthracis* and *Bacillus cereus* in the *gyrA* gene, a conserved region which has been previously difficult for other probes to discriminate (29). Probe design was accomplished through use of TP mathematical models, optimizing for maximum melting temperature differentials using a fixed linker length (a polyethylene glycol 9-mer) at an assay temperature of 40°C (1). Since the models are cooperative, combining elements of both linear probes and MBs, the same model could be used for the design of all the probes by simply setting the affinity of either the linear probe or the MB to zero. A 40°C assay temperature was chosen to reduce nonspecific adsorption and to help open up possible secondary structure in the targets that might affect the efficiency of binding. Higher temperatures were not used because, in general, the models predict larger melting temperature differentials for all probe types at lower temperatures than at higher temperatures. As expected, shortening the probes and/or increasing stem length produced predictions for lower melting temperatures and correspondingly larger melting temperature differentials. Synthesis of probes and template was performed by Biosearch Technologies (Novato, CA, USA). Table 1 contains a summary of probe and template sequences for five detection strategies including (i) labeled sample, (ii) sandwich assays using labeled linear probe, (iii) quantum dot labeled probe, (iv) MBs and (v) TPs. The same capture probe was used for all the detection strategies, except for the labeled sample (which used the quantum dot detection probe for a capture probe) because it did not contain dual probe specificity and needed to be designed around the SNP. Quantum Dots (Qdot 705 carboxylated) were purchased from Invitrogen, Carlsbad, California and were coupled to the corresponding detection probe (QDsand) following the Invitrogen protocol (<http://probes.invitrogen.com/media/pis/mp19020.pdf>), substituting primary amine terminated oligonucleotides wherever streptavidin is called for in the protocol. All probes were synthesized with deoxyribose nucleic acid chemistry.

Table 1. Probe sequences used in assay comparisons for each detection strategy

Detection strategy	Abbreviations	Sequence
Standard		
Capture probe	QDsand	CGCATGAcCATAT-T(C6-Amino)
Wild-type template	aLab	Q670-A(CGGTATACTTTCCCTTTATT)AGTGAAGAATAG(AATATGGTCAT) G(CGTAGAAGTGGTTAATAAATGCTCT)A-Q670
Variant template	cLab	Q670-A(CGGTATACTTTCCcTTATT)AGTGAAGAATAG(AATATGaTCAT) G(CGTAGAAGTGGTTAATAAATGCTCT)A-Q670
Sandwich		
Capture probe	CAPsand	(Amino-C6)T-AGAGCATTTATTAACCACTTCTACG
Linear probe	LINSand	Q670-CGCATGAcCATAT
Quantum Dot probe	QDsand	CGCATGAcCATAT-T(C6-Amino)
MB and TP sandwich		
Capture probe	CAPsand	(Amino-C6)T-AGAGCATTTATTAACCACTTCTACG
MB	MBSand	Q670-cCGCATGAcCATATTcgcgg-BHQ2
TP	TPsand	Q670-cgATGAcCATATTgcatcg-BHQ2-Spacer9(PEG) -AATAAAGGGAAAGTATA
Model targets		
Wild-type target	a	A(CGGTATACTTTCCCTTTATT)AGTGAAGAATAG(AATATGGTCAT) G(CGTAGAAGTGGTTAATAAATGCTCT)A
Near neighbor	c	A(CGGTATACTTTCCcTTATT)AGTGAAGAATAG(AATATGaTCAT) G(CGTAGAAGTGGTTAATAAATGCTCT)A
Alt. capture probe	CAPalt	(Amino-C6)T-AGAGCATTTATTAACCACTTCT

In sequence identity, the dash (-) represents a linkage to something other than a standard nucleotide, T(C6-amino) is a modified thymine base containing a 6-atom carbon chain with a primary amine terminus, Q670 is the fluorophore Quasar 670, BHQ2 is the Black Hole Quencher 2, Spacer 9 (PEG) is a nonaethylene glycol linker, parenthesis around nucleic acids show targeted regions for binding of capture and/or sandwich probes, lower case bases in the middle of probes or template represent the location of mismatches, nonbold lower case bases in MB and TP are bases added to help form the stem.

In order to allow a more direct comparison of probe technologies and detection methods, as many experimental variances were removed as possible. For this reason, purified synthetic template using a deoxyribose nucleic acid backbone was used in place of actual samples (removing potential variable interference from rRNA and nontargeted mRNA from total RNA sample preparation or from nonspecific amplicon in PCR preparation). The synthetic template used in the case of the standard labeled sample also removed variability in efficiency of the labeling step and in recovery of the sample. While limiting the number of labels to two fluorophores may affect the detection limit of the wild-type target, it is expected to affect the detection limit of the variant target in an equivalent manner. Template length is 71 bases, the size of a small amplicon.

Nonspecific adsorption

PPMs were synthesized in capillaries using a previously developed protocol (14). Briefly, after burning a 1–2 mm window in the teflon coating, capillaries were pretreated with a mixture of 0.4% v/v z-6030 silane in 2-propanol. The solution was used to fill the capillaries which were incubated for 15 min at 90°C. The monomer mixture contained 12.5% v/v 10 mM NaH₂PO₄, pH 7.2, 12.5% ethyl acetate, 40% methanol, 10.5% glycidyl methacrylate (GMA), 24.5% ethylene glycol dimethacrylate (EGDMA), also containing 30 mg/ml Irgacure (Ciba Specialty Chemicals, McIntosh, AL, USA). The solution was vortexed until the initiator was solubilized. The capillaries were then filled and photopolymerized at 365 nm using a UV crosslinking oven (Spectronics Corporation, Westbury, NY, USA) for 10 min.

Instead of functionalizing the PPM with nucleic acids, the epoxides were blocked with 100 mM of either propylamine, methoxy polyethylene glycol amine—750 (PEG), Tris-HCl (which possesses a primary amine and is potentially reactive with epoxides), or ethanolamine at 90°C for 1 h. Three capillaries of each were made. After blocking, one capillary volume (<1 µl) of 1 µM fluorescently labeled sample (wild-type target, aLab, in 10 mM Tris-HCl, pH 8.0, 200 mM NaCl, 0.1% Tween) was passed through the monolith at room temperature. The monolith was washed with 30 µl of wash buffer (10 mM Tris-HCl, pH 8.0, 200 mM NaCl, 0.1% Tween) at room temperature. Imaging was performed on a GenePix 4000a scanner by affixing the capillaries to a glass microscope slide. The gain settings were the same for all images.

Evaluation of capture probes

Two capture probes were made (CAPsand and CAPalt) differing by three bases on the 3'-end. There is a two-base overlap between the first capture probe (CAPsand) and sandwich probes (MBSand, LINSand, QDsand), which is expected to induce a slightly competitive reaction between the capture and detection probes, lowering the effective affinity and increasing the specificity relative to the reaction with the second capture probe (CAPalt). The two capture probes were evaluated for their effect on the wild-type and variant detection limits at 40°C by fluorescence measurement and melt curve analysis. Twenty microliters of 20-nM probe (TPsand, MBSand, LINSand), 100-nM target (a or c) and 1-µM capture probe (CAPsand or CAPalt) were analyzed in triplicate in an ABI 7500 PCR machine by performing a melt curve from 20°C to 60°C and fluorescent readout at 40°C.

The melting curve was conducted in 1°C incremental steps with 2 min incubation steps. The melting temperatures were approximated by the melting peak, which is the peak on the curve calculated as the change in fluorescence divided by the incremental change in temperature. QDsand was not used since Quantum Dots did not generate melt curves and because LINSand has the same probe sequence as QDsand. The capture probe resulting in the best separation of wild-type and variant detection limits (CAPsand) for all the probes was chosen for the remaining experiments.

PPM evaluation

Capillaries were prepared as described in Nonspecific adsorption section. An additional set of capillaries was prepared identically, except for GMA being used in place of EGDMA (i.e. no cross-linker was used, so no PPM was formed, only a surface layer of GMA). Both types were functionalized with CAPsand by covering the monolith with one capillary volume (<1 µl) of oligos in functionalization buffer (90 µM capture oligonucleotide, 2 mM PO₄ buffer pH 7.4, 600 mM NaCl) at 90°C for 1 h. No additional epoxide blocking was performed. Capillaries were loaded with different concentrations of 2 µl wild-type template for the standard assay (aLab, see Table 1) over 2 min at room temperature. They were washed with 10 µl of wash buffer over 2 min. The capillaries were imaged and lines were fit to the data. The intersection of the line with 3 SDs over background was considered the detection limit. Each data point was replicated on three different PPM containing capillaries.

Kinetics

PPMs were created in capillaries as described in Nonspecific adsorption section. They were functionalized with CAPsand by covering the monolith with one capillary volume (<1 µl) of oligos in functionalization buffer at 90°C for 1 h (as in PPM evaluation section). Blocking was performed as described previously, using 100 mM Tris-HCl, pH 8.0 at 90°C for 1 h.

The functionalized monoliths were loaded with one capillary volume (<1 µl) of 100 nM target (a) and were then loaded with 1 PPM volume (<1 µl, 20 nM) of either MBsand or TPSand at room temperature (24°C). Room temperature was used for monitoring the kinetics of the reaction because the TPs reacted too quickly to allow the heat transfer equipment (see Sensitivity and specificity section) to reach steady state prior to imaging. Imaging was performed as described previously (in Nonspecific adsorption section) over timed intervals. Three replicates were performed of each.

In an excess of target and for a forward rate constant much larger than the reverse rate constant, the rate equation can be described as (1):

$$F = F_{\max}(1 - e^{(-k_f T)t}) \quad 1$$

Where F is fluorescence, F_{\max} is the maximum fluorescence achieved at equilibrium, k_f is the effective forward rate constant, T is the target concentration and t is time. Each data set was best fit for the maximum fluorescence

Table 2. The steps for each detection strategy and the time in minutes

	Label sample	Load sample	Wash sample	Load probe	Hybridize probe	Wash probe	Total (min)
TPsand	0	2	0	1	2	0	5
MBsand	0	2	0	1	30	0	33
LINSand	0	2	0	1	2	2	7
QDsand	0	2	0	1	2	2	7
Standard	120 ^a	2	2	0	0	0	124

Total assay time is represented in the last column. Times given are the times input into the syringe pump's automated timer so no variances are included.

^aEstimate for time required to label the sample.

and the forward rate constant by minimizing the sum of square errors. The target concentration was set equal to the loaded concentration. The average rate constant was then computed for each probe type.

Sensitivity and specificity

PPMs were synthesized in capillaries functionalized with CAPsand or QDsand (for the standard labeled sample method) as described previously with no additional epoxide blocking step. To determine the appropriate flow rate, detection limits were determined for 0.1, 1.0 and 10.0 µl/min. Since the 1.0 µl/min flow rate produced optimal results, it was used for the experiments. In brief, 2 µl of nucleic acid sequences (either a or c) were passed through the capillary for 2 min at room temperature (24°C) in concentrations ranging from 100 pM to 1 mM. Afterwards, one PPM volume (<1 µl) of 20-nM probe (TPsand, MBsand, LINSand or Quantum Dot-labeled QDsand) was passed through the column and allowed to hybridize. TPSand and MBsand runs were immediately imaged and compared with a control run with no target. The other assays were first washed with 10 µl of wash buffer at 40°C and then imaged. All imaging was performed at 40°C by attaching a thermoelectric cooler to the underside of the microscope slide to which the capillary was affixed. A breakdown of each hybridization method with corresponding steps and time in minutes is listed in Table 2. Lines were fit to the average fluorescence versus target concentration. The intersection with 3 SDs over background was considered the detection limit. Each data point was replicated on three different PPM containing capillaries. Sensitivity in this paper is evaluated via the detection limit of the wild-type analyte. Specificity is evaluated through the ratio of the variant and wild-type detection limits.

RESULTS

The first set of experiments was performed to test nonspecific adsorption of labeled oligos to epoxide blocking agents (Figure 2). Propylamine, which presents a hydrophobic chemistry, was responsible for the largest amount of nonspecific adsorption. Ethanolamine, a common epoxide blocking reagent, also caused considerable adsorption. The unblocked PPM and hydrophilic blocking reagents caused the least amount of adsorption.

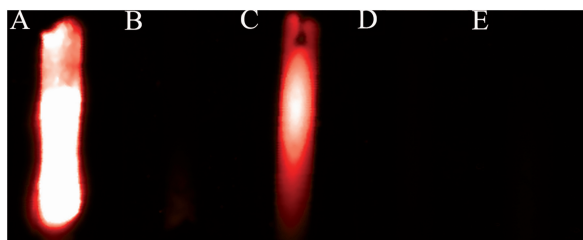


Figure 2. Nonspecific adsorption of labeled oligonucleotides in representative PPM containing capillaries where the unreacted epoxides were blocked with propylamine (A), methoxy PEG amine (B), ethanolamine (C) and Tris-HCl (D), versus a control PPM with no epoxide blocking (E). PPM segments are $\sim 250\ \mu\text{m}$ diameter by 1.5 mm length.

Table 3. Melting temperatures (in $^{\circ}\text{C}$) for wild-type (WT) and variant (Var) using either of two probes, CAPsand or CAPalt in conjunction with the sandwich probes

Probe	CAPsand			CAPalt		
	WT T_m	Var T_m	ΔT_m	WT T_m	Var T_m	ΔT_m
TPsand	40	<20	>20	39	<20	>19
MBsand	48	<20	>28	54	42	12
LINsand	49	34	15	53	40	13

Once the effectiveness of each blocking agent had been established, each capture probe was evaluated. MBs and TPs are amenable to melt curves, and the findings of Crockett and Wittwer (30) have demonstrated that even single labeled probes can be used for melt curve analysis, so melt curves were used for the capture probe evaluation. Table 3 summarizes the melting peak data, which is obtained from the first derivative of the melting curve data. The difference between the wild-type and variant melting peaks is an indication of the quality of the probe. A set of wild-type and variant melting peaks that are centered about the reaction temperature and have a greater temperature differential are generally less likely to have false positives or negatives. Since melting temperature differentials obtained with CAPsand were larger than those obtained with CAPalt and also surrounded the desired reaction temperature of 40°C , CAPsand was used for the remaining experiments.

PPMs functionalized with CAPsand were evaluated for their effect on the detection limit in comparison with capillaries with no PPM. The detection limit of capillaries without PPM was $154\ \text{pM}$ labeled wild-type target, in contrast to the detection limit of $7.7\ \text{pM}$ for capillaries with PPM. Since the PPM improved the detection limit by 20-fold, it was used for the evaluation and comparison of the various hybridization-based detection strategies.

Prior to performing the sandwich assays, MB and TP kinetics were analyzed. The rate of TP reaction is visibly faster than that of the MBs and was further quantified by extracting rate constants from the fitted curves (Figure 3). TPs had a time constant ($\tau = 1.25\ \text{min}$) that was 37.6 times faster than the MB time constant ($\tau = 47\ \text{min}$). Although the rates of the MBs in the reaction appear slow, the fitted

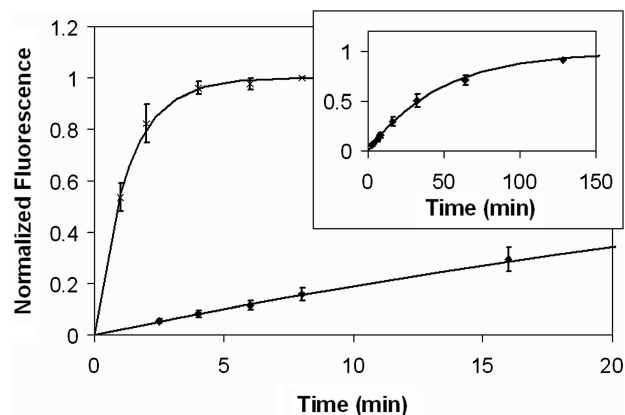


Figure 3. Kinetics of TP (x) versus MB (diamonds) in a sandwich assay hybridization (100-nM template, 20-nM probe). The inset shows extended MB performance out to 150 min. Three replicates were run on different capillaries. Curves were fit to Equation (1).

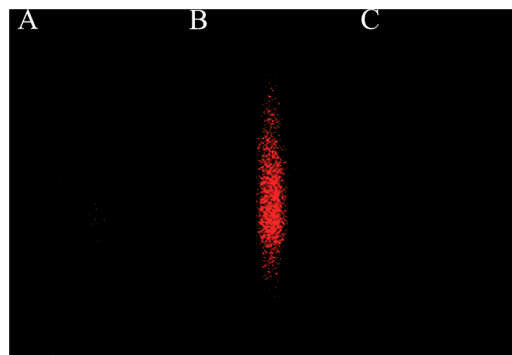


Figure 4. TP sandwich assay for $2\ \mu\text{l}$ 100 pM wild-type target injected over 20 min before adding TPs (A), after adding TPs (B) and a control with TPs and no target (C). PPM segments are $\sim 250\ \mu\text{m}$ diameter by 1.5-mm length.

rate constant of $3500\ \text{M}^{-1}\ \text{s}^{-1}$ compares favorably to other MB rate constants in literature (23). The TP rate constant of $133\ 000\ \text{M}^{-1}\ \text{s}^{-1}$ was also similar to previously reported rates in solution (1). The data from this experiment was used to determine that the MBs required more than the 2 min allotted for the other assays to fully react (see Table 2 for hybridization probe incubation times). In the remainder of the experiments, the MBs were given 30 min to react.

With the PPM characterized and the probe hybridization times optimized, we were prepared to test the sandwich assay (Figure 4 shows a representative example of a TP assay). A comparison of the detection limits of wild-type and variant target for each detection strategy revealed some unique advantages of TPs (Figure 5). TPs not only achieved equivalent or better detection limit ($P = 0.034$, t -test against overall probe performance), but they were also the only probes to significantly improve specificity ($P = 0.000\ 058$), with over four orders of magnitude improvement over the other probe types. In fact when a slightly higher threshold (6 SD above background) was applied, no false positives occurred for TPs at any concentration tested (tested up to 1 mM). All of the other

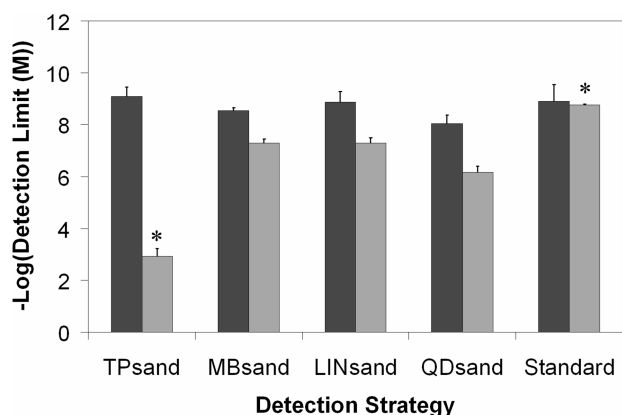


Figure 5. Absolute value of the log of the wild-type detection limit (dark gray bars) and variant detection limit (light gray bars) of five different detection strategies. In each case, 2- μ l sample was loaded at a flow rate of 1 μ l/min. Significant results (*) using Bonferroni correction for *t*-test are shown. Ratio of variant to wild-type detection limits indicates 10000-fold improvement in specificity for TPs (1×10^6) over other probe types (10–100).

probes experienced false positives at variant concentrations <100-fold, greater than the wild-type detection limit.

DISCUSSION

Hybridization assays require a combination of speed, sensitivity and specificity. Here we examined how PPM affects the speed of the assay and how TPs increase specificity in sandwich assays with similar or better sensitivity than other probe technologies.

The speed of an assay is heavily influenced by the hybridization time. Microfluidic assays enhance the reaction time by adding convection to the system and by decreasing diffusion distances. Porous substrates decrease the diffusion distance even further while simultaneously increasing the surface area, hence the possible concentration of probes affixed to the surface, which increases the probability of a collision and a subsequent reaction between probe and target. PPMs provide a good porous substrate as their pore size is readily controlled by the amount and composition of the porogenic solvent. Their surface chemistries are readily modified by incorporation of methacrylates with the desired functionality. Epoxides are one surface chemistry which allow modification with many types of biomolecules. By modifying PPM with oligonucleotides, we were able to improve the detection limits of an assay by almost 20-fold using only 2 μ l of sample.

One method of decreasing the assay time is to bypass some of the standard steps. Zuo *et al.* (18) claimed that using MBs in a sandwich assay enabled them to bypass the wash step without sacrificing the detection limit. However, the kinetics of the reaction were not discussed. Here we show that for a typical MB the hybridization reaction takes 47 min ($\tau = 47$ min). Thus, most of the time saved in bypassing the wash step is lost in the kinetics of the probe hybridization. In contrast, the TP reaction took 1.25 min, demonstrating the more rapid kinetics of TPs compared to MBs in sandwich assays. This also demonstrates that

TP hybridization at the solution-surface interface maintains the kinetic advantages TPs have shown over MBs in free solution (1).

The speed at which TPs react may seem counterintuitive. The 6-base loop domain of the detection region would appear too small and too specific (i.e. because of the strong stem) to react quickly. However, the cooperative interaction between the capture and detection regions increases the rate at which TPs react. The relatively long-capture region increases the overall probe size above that of a MB, increasing the probability of a collision with the target. The linear capture region is able to react quickly with the target, which it then holds proximal to the detection region, forcing a reaction that might not otherwise occur. While synthetic targets were used in this work, the same kinetic advantage stemming from cooperativity should apply toward any target where the linear capture region is able to bind quickly and efficiently.

Hybridization kinetics not only determine the speed of an assay, but may also impact the detection limit if the reaction is not allowed to proceed to completion before imaging. TPs had a lower detection limit ($P = 0.022$) than MBs. This could be due to the fact that MBs react slower and are not finished reacting even after 30 min. It could also be due to the lower avidity of MBs for their target. In order to maintain adequate specificity, a MB must be designed with relatively low affinity toward its target. While larger loops or shorter stems may increase both the affinity and the rate at which a MB reacts, there is a tradeoff in signal to noise and in specificity. A TP, however, is a cooperative probe and can be designed with a high affinity in the capture region for capture of the target and low affinity in the detection region for enhanced specificity (the low-melting temperature shown in Table 3 is an effective melting temperature and reflects the state at which the detection region is half bound, the capture region is still capable of binding at temperatures far above where the detection region melts off, increasing the avidity of the probe).

As discussed previously, affinity affects the detection limit of the assay. Unfortunately, a high affinity towards the wild-type target usually corresponds to a low specificity because a heightened affinity will also be exhibited toward variant sequences. In order to make the standard labeled sample assay more specific, the probe length was shortened and designed around the SNP. This action increased the stringency (i.e. the conditions necessary for probe target hybridization to occur, supposedly simultaneously decreasing the probability that nonspecific reactions will occur) of the assay sufficiently that 90% of the bound target eluted during the 10 μ l wash step (data not shown). However, even with such a high stringency, when the variant was concentrated to high levels, it bound to the PPM nearly as abundantly as the wild-type. This is a problem with labeling the sample instead of using a more specific method. When the specificity of an assay depends entirely upon a single probe, it has to be made extremely specific, which prevents the wild-type from being pre-concentrated (compare 2 nM detection limit using QDSand to 7 pM detection limit using CAPsand, where the only change is the strength of the capture probe). Not only is

the wild-type not adequately preconcentrated, but it is also heavily eluted from the PPM during the wash step, preventing more rigorous wash steps. Thus, when high concentrations of variant are encountered (>100 nM), the short wash step is not sufficient to remove all of the variant adsorbed to the PPM, causing the variant detection limit to appear similar (within an order of magnitude) to the wild-type detection limit which in turn was somewhat greater (less sensitive) than would be expected.

Every sandwich assay in this experiment had greater specificity than the standard labeled sample assay while maintaining nearly equivalent wild-type detection limits ($P = 0.00027$, t -test of standard labeled probe against average probe performance). This is because the capture probe on the PPM could be made with a high affinity so as to not elute the target. The specificity could then be achieved by adding a labeled, specific oligonucleotide that targets only the wild-type. Further, the concentration of the label was controllable, since a small (20 nM), fixed amount of probe was added to the PPM every time.

The wild-type detection limits of the assays were generally the same (~ 1 nM). However, as expected, the quantum dot-labeled oligos performed relatively poorly ($P = 0.017$, t -test against average probe performance). Quantum dots do not photo-bleach and have a large Stokes shift; however, under the excitation conditions used by the Gene Pix 4000a scanner (532 and 635 nm) quantum dots have a relatively small molar absorptivity and quantum yield in comparison with organic dyes. Since the optical properties of the quantum dots were the same for both wild-type and variant samples, the use of quantum dots on the Gene Pix scanner still provided for an accurate measure of the ratio between variant and wild-type detection limits. In spite of the poor wild-type detection limit of the quantum dot assay, it had a better specificity than the other probe types with the exception of the TPs. This was again surprising as the detection probe used in the quantum dot assay is the same as the one used in the linear probe sandwich assay. However, the quantum dot seemed to exhibit a lesser affinity for the PPM than the hydrophobic dye-labeled oligos, as the background for the quantum dot assays with no template returned almost to the original fluorescence when washed.

TPs possessed the lowest detection limit and the highest specificity. Since TPs exhibit an inherent background due to nonquenched fluorescence and since the probe used in this work had a melting temperature equivalent to the reaction temperature, it may be thought that they would be less sensitive than the other methods. However, the rapidity with which they react and their high affinity appear to be sufficient to yield a large signal. Also, since the TP reaction has no need of a wash step, no wild-type target is lost. All of this together gives a relatively sensitive sandwich assay, notwithstanding the fact that the probe is only half reacted at 40°C .

However, of perhaps greater importance is the concentration-independent specificity of the TP assay. Although the wild-type and variant targets differ by only a single nucleotide polymorphism in an 'AT' rich region, the TP is not only able to discriminate, but is also able to do so across more than six orders of magnitude

of concentrations (more than four orders of magnitude greater than any of the other probes). This behavior and the fast kinetics are properties that were shown to be exclusively possessed by TPs in free solution (1). However, this is the first application of TPs in a surface reaction, and it is apparent that their attributes apply equally well at the surface as they do in free solution.

Concentration-independent specificity means that the behavior of the hybridized probe does not change with increasing concentrations of nucleic acids. Thermodynamics dictate that every probe is concentration dependent. However, TPs use cooperativity to generate a pseudo-concentration independence. This is achieved by utilization of a capture region with a higher affinity than that of the detection region. If the target or variant concentration is much greater than the concentration of the capture region, the capture region is saturated with target presenting a constant local concentration to the detection region which is independent of how much target is added to the solution. In surface-bound assays, including sandwich assays, concentration-independent specificity could be very useful. In a PCR reaction, specificity is only necessary over one to two orders of magnitude of template concentrations as the primer concentration gives an upper bound to the concentrations seen and the polymerase amplifies the reaction to a detectable level. In surface-bound assays with conventional probes, the probe must be sufficiently avid so that it binds the target sequence (picomolar) while binding weakly (weaker than micromolar) to all near neighbors so that they are removed in the wash step. Sandwich assays somewhat improve this by allowing stronger avidity for the near neighbors before the wash, but the probe must still detect a relatively small number of target sequences among orders-of-magnitude more near neighbors (perhaps as many as millions more if avidity is almost equal in the capture step of the assay). Here, we present a possible solution to the concentration dependence of hybridization probe technologies in surface-based assays. TPs have shown specificity over six orders of magnitude of concentrations. While more sensitive detectors will need to be developed in order to truly bypass PCR, we feel that the specificity of TPs over such a large range of concentrations in surface-based hybridization assays will help in the overall accomplishment of that goal.

In addition to the sensitivity and specificity of the TP assay, it also had the fastest overall assay time of 5 min. While the MB assay was also able to bypass the wash step, it did so at the cost of a 30-min hybridization step. The standard labeled sample took a long time because, although the assay is simple to perform, the sample preparation time is much larger due to the necessity of labeling the sample.

Also noteworthy are the fast reaction time and small volumes of the PPM. The reactions in the PPM required only $2\ \mu\text{l}$ and took place in 2 min. This is in contrast to a MB sandwich assay recently performed that required 30 min for hybridization of $2\ \mu\text{l}$ (18). The small sample size implies reduced costs and the potential to use higher concentrations, thereby decreasing the probability of false negatives.

While this study utilized synthetic templates in order to examine the unbiased performance of each probe type and of the PPM, further study using real samples may reveal additional characteristics of each probe type and of the PPM in general. Various stratagems have been employed for the production of short, single-stranded oligos for hybridization such as bead-based magnetic separation of PCR strands, asymmetric PCR, enzyme degradation of complementary strands and heat or alkaline denaturation of strands (31–35). A complete analysis of these methods and others is beyond the scope of this work. However, these methods have been reviewed and compared in connection with microarray hybridization studies (36). As the primary difference between these studies and our own is the solid support (i.e. the PPM), we would expect similar hybridization trends on the PPM.

Specifically, we expect any of the foregoing methods involving PCR amplification of target that results in a relatively short amplicon (the targets used in our studies were 71 bases in length), where the targeted strand has been enriched (similar to using single-stranded target in our experiments) to exhibit similar performance to what was shown in this work. We would also expect that the extraction and subsequent detection of mRNA or other single-stranded targets would have similar performance to what was done in this work. In support of this statement, up to 16 µg of mRNA (mRNA ranges from several hundred to several thousand bases in length) was extracted with high efficiency from total RNA on identical PPMs functionalized with oligo dTs under even faster flow conditions (5 µl/min) (14). Another important consideration in developing PPMs as a diagnostic tool will be the overall sensitivity. The nanomolar detection limits exhibited by the assays in this work are adequate for post-PCR concentrations, but will not be sufficient for detection of many biological samples without amplification. In considering the suitability of the PPM as a detection scaffold, it should be noted that the wild-type detection limits of the assays performed in this article may have been hindered by the detection method. Principally, the GenePix 4000a scanner is not designed for scanning capillaries. The focus of both laser and optics are on the plane of the slide, reducing the signal and increasing the amount of expected scatter from the capillary attached to its surface. Optimization of the focal plane could potentially increase the detection limits. Further, since the PPM is designed to extract and concentrate the analyte, larger sample volumes could be used to preconcentrate the analyte to detectable levels.

In conclusion, utilization of the PPM for direct detection of nucleic acids has appeal as it provides a large surface area for the rapid adsorption and efficient extraction of specific nucleic acid sequences. Reaction times of 2 min and enhancements in detection limits of 20-fold from only 2 µl indicate its potential in the field of surface-based detection. Further, we have compared five different detection strategies in the PPM and have shown that TPs complement the rapidity of extraction of the PPM with fast kinetics, with good sensitivity, and with concentration-independent specificity, providing more than six orders of magnitude of selectivity.

FUNDING

National Institute of Dental and Craniofacial Research Career Development and Faculty Transition Award (K22 DE014846 to M.R.C.); National Institute of Health Exploratory Research Grant R21 (NS510386 to M.R.C.); U.S. Department of Homeland Security Scholarship and Fellowship Program (DE-AC05-00OR22750 to B.C.S.); Small Business Innovative Research grant (NBCHC060031 to Arcxis Biotechnologies). Funding for open access charge: Arizona State University.

Conflict of interest statement. All opinions expressed in this article are the authors' and do not necessarily reflect the policies and views of DHS, DOE or ORISE.

REFERENCES

- Satterfield, B.C., West, J.A. and Caplan, M.R. (2007) Tentacle probes: eliminating false positives without sacrificing sensitivity. *Nucleic Acids Res.*, **35**, e76.
- Kohara, Y., Noda, H., Okano, K. and Kambara, H. (2002) DNA probes on beads arrayed in a capillary. 'Bead-array', exhibited high hybridization performance. *Nucleic Acids Res.*, **30**, e87.
- Cheek, B.J., Steel, A.B., Torres, M.P., Yu, Y.Y. and Yang, H. (2001) Chemiluminescence detection for hybridization assays on the flow-thru chip, a three-dimensional microchannel biochip. *Anal. Chem.*, **73**, 5777–5783.
- Beuningen, R., Damme, H., Boender, P., Bastiaensen, N., Chan, A. and Kievits, T. (2001) Fast and specific hybridization using flow-through microarrays on porous metal oxide. *Clin. Chem.*, **47**, 1931–1933.
- Dufva, M., Petronis, S., Jensen, L.B., Krag, C. and Christensen, C.B. (2004) Characterization of an inexpensive, nontoxic, and highly sensitive microarray substrate. *Biotechniques*, **37**, 286–292, 294, 296.
- Yu, C., Davey, M.H., Svec, F. and Frechet, J.M. (2001) Monolithic porous polymer for on-chip solid-phase extraction and preconcentration prepared by photoinitiated in situ polymerization within a microfluidic device. *Anal. Chem.*, **73**, 5088–5096.
- Shediach, R., Ngola, S.M., Throckmorton, D.J., Anex, D.S., Shepodd, T.J. and Singh, A.K. (2001) Reversed-phase electrochromatography of amino acids and peptides using porous polymer monoliths. *J. Chromatogr. A*, **925**, 251–263.
- Throckmorton, D.J., Shepodd, T.J. and Singh, A.K. (2002) Electrochromatography in microchips: reversed-phase separation of peptides and amino acids using photopatterned rigid polymer monoliths. *Anal. Chem.*, **74**, 784–789.
- West, J.A.A., Hukari, K.W., Hux, G. and Shepodd, T.J. (2004) Microfluidic gene arrays for rapid genomic profiling. *Proceedings of the Society of Photo-Optical Instrumentation Engineers (SPIE) Conference on Lab-on-a-Chip: Platforms, Devices, and Applications; 26–28 October 2004; Philadelphia, PA*, **5591**, pp. 167–173.
- Svec, F., Tennikova, T.B. and Deyl, Z. (eds.) (2003) *Monolithic Materials: Preparation, Properties, and Applications*. Elsevier, Amsterdam.
- Yu, C., Xu, M.C., Svec, F. and Frechet, J.M.J. (2002) Preparation of monolithic polymers with controlled porous properties for microfluidic chip applications using photoinitiated free-radical polymerization. *J. Polym. Sci., A*, **40**, 755–769.
- Ngola, S.M., Fintschenko, Y., Choi, W.Y. and Shepodd, T.J. (2001) Conduct-as-cast polymer monoliths as separation media for capillary electrochromatography. *Anal. Chem.*, **73**, 849–856.
- West, J.A.A. and Satterfield, B.C. (2007) Fabrication of porous polymer monoliths in microfluidic chips for selective nucleic acid concentration and purification. In Floriano, P.N. (ed.), *Microchip-Based Assay Systems: Methods and Applications*. Humana Press Inc., Totowa, NJ, pp. 9–21.
- Satterfield, B.C., Stern, S., Caplan, M.R., Hukari, K.W. and West, J.A. (2007) Microfluidic purification and preconcentration of mRNA by flow-through polymeric monolith. *Anal. Chem.*, **79**, 6230–6235.

15. Dunn,A.R. and Hassell,J.A. (1977) A novel method to map transcripts: evidence for homology between an adenovirus mRNA and discrete multiple regions of the viral genome. *Cell*, **12**, 23–36.
16. Ranki,M., Palva,A., Virtanen,M., Laaksonen,M. and Soderlund,H. (1983) Sandwich hybridization as a convenient method for the detection of nucleic acids in crude samples. *Gene*, **21**, 77–85.
17. Syvanen,A.C., Tchen,P., Ranki,M. and Soderlund,H. (1986) Time-resolved fluorometry: a sensitive method to quantify DNA-hybrids. *Nucleic Acids Res.*, **14**, 1017–1028.
18. Zuo,X., Yang,X., Wang,K., Tan,W. and Wen,J. (2007) A novel sandwich assay with molecular beacon as report probe for nucleic acids detection on one-dimensional microfluidic beads array. *Anal. Chim. Acta*, **587**, 9–13.
19. Drake,T.J. and Tan,W. (2004) Molecular beacon DNA probes and their bioanalytical applications. *Appl. Spectrosc.*, **58**, 269A–280A.
20. Marras,S.A., Kramer,F.R. and Tyagi,S. (2002) Efficiencies of fluorescence resonance energy transfer and contact-mediated quenching in oligonucleotide probes. *Nucleic Acids Res.*, **30**, e122.
21. Tyagi,S. and Kramer,F.R. (1996) Molecular beacons: probes that fluoresce upon hybridization. *Nat. Biotechnol.*, **14**, 303–308.
22. Bonnet,G., Tyagi,S., Libchaber,A. and Kramer,F.R. (1999) Thermodynamic basis of the enhanced specificity of structured DNA probes. *Proc. Natl Acad. Sci. USA*, **96**, 6171–6176.
23. Tsourkas,A., Behlke,M.A., Rose,S.D. and Bao,G. (2003) Hybridization kinetics and thermodynamics of molecular beacons. *Nucleic Acids Res.*, **31**, 1319–1330.
24. Mammen,M., Choi,S. and Whitesides,G.M. (1998) Polyvalent interactions in biological systems: implications for design and use of multivalent ligands and inhibitors. *Angew. Chem. Int. Ed.*, **37**, 2754–2794.
25. Kiessling,L.L., Gestwicki,J.E. and Strong,L.E. (2000) Synthetic multivalent ligands in the exploration of cell-surface interactions. *Curr. Opin. Chem. Biol.*, **4**, 696–703.
26. Chung,Y.C., Jan,M.S., Lin,Y.C., Lin,J.H., Cheng,W.C. and Fan,C.Y. (2004) Microfluidic chip for high efficiency DNA extraction. *Lab Chip*, **4**, 141–147.
27. Handl,H.L., Vagner,J., Han,H., Mash,E., Hruby,V.J. and Gillies,R.J. (2004) Hitting multiple targets with multimeric ligands. *Expert Opin. Ther. Targets*, **8**, 565–586.
28. Caplan,M.R. and Rosca,E.V. (2005) Targeting drugs to combinations of receptors: a modeling analysis of potential specificity. *Ann. Biomed. Eng.*, **33**, 1113–1124.
29. Satterfield,B.C., Kulesh,D.A., Norwood,D.A., Wasieloski,L.P. Jr, Caplan,M.R. and West,J.A. (2007) Tentacle Probes™: differentiation of difficult single-nucleotide polymorphisms and deletions by presence or absence of a signal in real-time PCR. *Clin. Chem.*, **53**, 2042–2050.
30. Crockett,A.O. and Wittwer,C.T. (2001) Fluorescein-labeled oligonucleotides for real-time pcr: using the inherent quenching of deoxyguanosine nucleotides. *Anal. Biochem.*, **290**, 89–97.
31. Espelund,M., Stacy,R.A. and Jakobsen,K.S. (1990) A simple method for generating single-stranded DNA probes labeled to high activities. *Nucleic Acids Res.*, **18**, 6157–6158.
32. Gyllensten,U.B. and Erlich,H.A. (1988) Generation of single-stranded DNA by the polymerase chain reaction and its application to direct sequencing of the HLA-DQA locus. *Proc. Natl Acad. Sci. USA*, **85**, 7652–7656.
33. Higuchi,R.G. and Ochman,H. (1989) Production of single-stranded DNA templates by exonuclease digestion following the polymerase chain reaction. *Nucleic Acids Res.*, **17**, 5865.
34. Wang,R.F., Beggs,M.L., Robertson,L.H. and Cerniglia,C.E. (2002) Design and evaluation of oligonucleotide-microarray method for the detection of human intestinal bacteria in fecal samples. *FEMS Microbiol. Lett.*, **213**, 175–182.
35. Riccelli,P.V., Merante,F., Leung,K.T., Bortolin,S., Zastawny,R.L., Janeczko,R. and Benight,A.S. (2001) Hybridization of single-stranded DNA targets to immobilized complementary DNA probes: comparison of hairpin versus linear capture probes. *Nucleic Acids Res.*, **29**, 996–1004.
36. Gao,H., Tao,S., Wang,D., Zhang,C., Ma,X., Cheng,J. and Zhou,Y. (2003) Comparison of different methods for preparing single stranded DNA for oligonucleotide microarray. *Anal. Lett.*, **36**, 2849–2863.